MABS
2016, VOL. 8, NO. 7, 1210–1223
http://dx.doi.org/10.1080/19420862.2016.1204502

Taylor & Francis
Taylor & Francis Group

REPORT

OPEN ACCESS

In-depth structural characterization of Kadcyla® (ado-trastuzumab emtansine) and its biosimilar candidate

Liuxi Chen[a,*], Lan Wang[b,*], Henry Shion[a], Chuanfei Yu[b], Ying Qing Yu[a], Lei Zhu[c], Meng Li[b], Weibin Chen[a], and Kai Gao[b]

[a]Waters Corporation, Milford, MA, USA; [b]National Institutes of Food and Drug Control, Tiantan Xili, Beijing, P.R. China; [c]Second Military Medical University, International Joint Cancer Institute, Shanghai, China

ASBTRACT

The biopharmaceutical industry has become increasingly focused on developing biosimilars as less expensive therapeutic products. As a consequence, the regulatory approval of 2 antibody-drug conjugates (ADCs), Kadcyla® and Adcetris® has led to the development of biosimilar versions by companies located worldwide. Because of the increased complexity of ADC samples that results from the heterogeneity of conjugation, it is imperative that close attention be paid to the critical quality attributes (CQAs) that stem from the conjugation process during ADC biosimilar development process. A combination of physicochemical, immunological, and biological methods are warranted in order to demonstrate the identity, purity, concentration, and activity (potency or strength) of ADC samples. As described here, we performed extensive characterization of a lysine conjugated ADC, ado-trastuzumab emtansine, and compared its CQAs between the reference product (Kadcyla®) and a candidate biosimilar. Primary amino acid sequences, drug-to-antibody ratios (DARs), conjugation sites and site occupancy data were acquired and compared by LC/MS methods. Furthermore, thermal stability, free drug content, and impurities were analyzed to further determine the comparability of the 2 ADCs. Finally, biological activities were compared between Kadcyla® and biosimilar ADCs using a cytotoxic activity assay and a HER2 binding assay. The in-depth characterization helps to establish product CQAs, and is vital for ADC biosimilars development to ensure their comparability with the reference product, as well as product safety.

Abbreviations: ADC, antibody-drug conjugate(s); CQAs, critical quality attributes; DARs, drug-to-antibody ratios; mAb, monoclonal antibody; FDA, Food and Drug Administration; DM1, emtansine; DSC, Differential scanning calorimetry; SEC, size-exclusion chromatography; SMCC, succinimidyl 4-(N-maleimidomethyl) cyclohexane-1-carboxylate; CE-SDS, Capillary sodium dodecyl sulfate gel electrophoresis; SPR, Surface plasmon resonance; XIC, extracted ion chromatographic; CDR, complementarity-determining region; DDA, data dependent acquisition; UV/Vis, ultraviolet-visible spectrophotometry; MALDI-TOF-MS, Matrix-assisted laser desorption/ionization time-of-flight mass spectrometry; CE-MS, capillary electrophoresis–mass spectrometry; HIC, hydrophobic interaction chromatography; IMMS, ion mobility mass spectrometry; ESI-MS, electrospray ionization mass spectrometry

ARTICLE HISTORY
Received 28 March 2016
Revised 14 June 2016
Accepted 17 June 2016

KEYWORDS
Antibody-drug conjugates; biosimilar; immunoconjugates; LC/MS; peptide mapping

Introduction

Antibody-drug conjugates (ADCs) or immunoconjugates are a sub-class of biotherapeutics designed to facilitate the targeted delivery of potent cytotoxic drugs to cancer cells. The creation of ADC molecules as a therapeutic modality realized, to a certain degree, a long-standing wish for a "magic bullet" that could be harnessed to deliver cytotoxic therapy directly to the source of the disease.[1] ADCs are composed of a cytotoxic drug linked to a monoclonal antibody (mAb) via a chemical linker. The combination takes advantage of the enhanced selectivity of mAbs targeting cancer-specific antigens, and utilizes highly potent cell-killing agents that are otherwise too toxic to develop as therapeutics by minimizing systemic toxicity. ADCs have recently shown promise in the treatment of various cancers.[2] Many novel ADCs are currently in preclinical, early clinical or late-stage clinical development for the treatment of solid and hematologic tumors.[3,4] Two ADC drugs were approved recently by the US Food and Drug Administration (FDA), brentuximab vedotin (Adcetris®, Seattle Genetics), and ado-trastuzumab emtansine (Kadcyla®, Genentech). The commercial success of ADCs has generated interest in the development of novel and biosimilar ADCs across the biopharmaceutical industry.

Depending on the conjugation chemistry, different types of ADCs can be constructed, e.g., cysteine-conjugated, lysine-conjugated or site-specific ADCs.[5,6] It is important to note that the degree of heterogeneity of the ADC varies with the strategy used for conjugating the drug (through the linker) to the antibody. At a molecular level, all ADC molecules bear complex chemical structures, combining the molecular characteristics of small-molecule drugs with those of large molecule mAbs. In addition, the conjugation reaction employed for the synthesis

CONTACT Weibin Chen weibin_chen@Waters.com; Kai Gao gaokai@nifdc.org.cn
*These authors equally contributed to this work.

of ADCs increases the complexity of ADC samples to a higher level by producing a mixture of ADC molecules that are heterogeneous in 2 regards. First, the product population contains conjugates in a range of different drug-to-antibody ratios (DARs). For example, with conjugation at lysine residues, a distribution of DARs ranging from 0 to 8 drugs has been reported.[7] Second, any 2 conjugates with the same DAR are likely regio-isomers because the conjugation reaction is typically a random process, and there are many surface-accessible lysine residues (as well as the N termini of the light and heavy chains) in the mAb as potential candidates for modification. For example, one study found that a lysine-conjugated ADC sample with DARs ranging from 0 to 6 potentially contains over 4.5 million unique molecules.[8] Partial modification at those accessible lysine residues results in a population of products differing in conjugation sites. In contrast, the heterogeneity for cysteine-conjugated ADC samples is significantly less because there are at most 8 cysteine conjugation sites available (for IgG1). Consequently, physical/chemical properties vary with the degree of heterogeneity of the ADC, which determines the analysis strategy used for characterizing the ADC and ensuring the ADC product quality.

Given the outcome of conventional ADC manufacturing methods, the clinically approved ADCs were developed and administered as heterogeneous mixtures. This heterogeneity presents challenges to both the analysis of ADC structures, product quality and manufacturing consistency. To gain an in-depth understanding of ADC structures and product quality, thereby establishing better quality control of the final drug product, various analytical techniques have been developed. For example, different analytical approaches have been employed to study ADCs at the intact protein level, the sub-domain level, and the individual peptide level.[9-13] Although these analytical techniques are the same tools used for other biopharmaceuticals (e.g., mAbs), some specific methods were needed because of the structural complexity of ADCs and the presence of their cytotoxic agents. As a result, a substantial number of methods for the physicochemical characterization of unique features of ADCs have been developed. These include methods used in the characterization of drug-load profile and distribution,[14-16] the average DAR,[17,18] the conjugation sites,[8,19] and the amount of unconjugated payload-related species.[20] The continuous reports of this research highlight the fact that no single technique can satisfactorily provide sufficient information about the ADC molecules. However, while physicochemical techniques can produce information about structure and composition and are used to monitor content, purity, and chemical stability of ADC, physicochemical techniques cannot yet predict ADC biological activity. Thus, a combination of physicochemical, immunological, and biological methods is necessary to demonstrate the identity, purity, concentration, and activity (potency or strength) of ADC samples.

There has been increasing interest by the biopharmaceutical industry in the development of biosimilars (including mAbs and ADCs) in order to bring less expensive biotherapeutics to the world market.[21] The clinical and commercial successes of Kadcyla® and Adcetris® validated ADCs as a therapeutic approach, but also prompted substantial interest in developing biosimilar versions. Due to the increasing level of ADC sample complexity that comes with the heterogeneity of their conjugations, some critical quality attributes (CQAs) are unique to this type of molecules. These CQAs are linked to the conjugation process and deserve both recognition and close attention when assessing ADC biosimilars. They include the drug distribution, average DAR, drug-related impurities, potency, amount of unconjugated mAb, conjugation sites and site occupancy, to name a few. These ADC product CQAs are directly linked to target site specificity, binding properties, and the in vitro and in vivo stability of the linker and drug, which in turn determines both the clinical efficacy and safety of an ADC.[22] Because of the intrinsic complexity, the CQAs can only be acquired through extensive characterization of ADCs via a combination of physicochemical, immunological, and biological methods. The establishment of the CQAs is vital for developing biosimilar ADCs to ensure their comparability with the reference (i.e., brand) product and product safety.

The FDA approved ado-trastuzumab emtansine for the treatment of human epidermal growth factor receptor (HER)2-positive breast cancer under the brand name Kadcyla® in 2013. Kadcyla® consists of the therapeutic anti-HER2 antibody trastuzumab, marketed under the brand name Herceptin®, covalently linked to a maytansine derivative (DM1) via a linker (Fig. 1). The lysine-conjugated ADCs, like Kadcyla®, utilize the solvent-exposed ε-amino groups of lysine residues to attach drugs. Trastuzumab contains 88 lysines and 4 N-terminal groups that could be modified through the conjugation steps. Due to the heterogeneous nature of lysine conjugation chemistry, the resulting conjugates consist of subpopulations that differ in the number of drugs attached, as well as the location of the drug linkage. Previous studies with Kadcyla® or other antibody-DM1 conjugates have given some insight into the drug distribution, load and location of conjugation sites.[8,19] A report on Kadcyla® suggests that an average of ~3.5 DM1 molecules are conjugated to every trastuzumab molecule, and at least 70 lysine sites are partially conjugated with the drug.[7] However, the list of conjugation sites and relative site occupancy has not been described, and the effects of the lysine conjugation sites

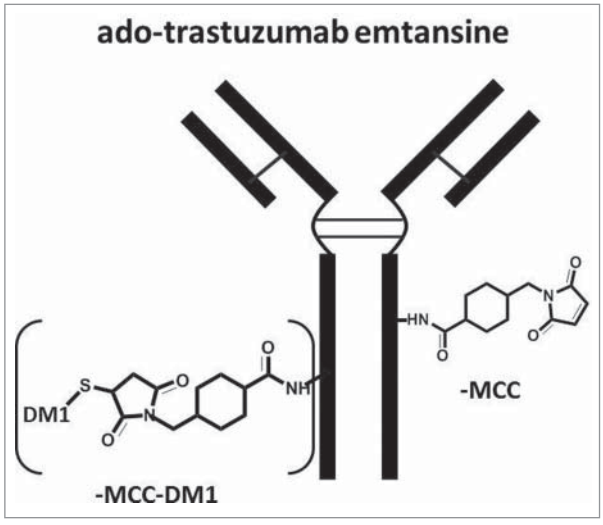

Figure 1. Schematic of ado-trastuzumab emtansine conjugation. Modification of lysines on trastuzumab with SMCC linker and subsequent reaction with sulfhydryl of the DM1 drug. MCC-DM1 represents the linker with the DM1 drug and MCC represents the linker. MCC-DM1 = 956.3644, MCC = 219.0895.

and relative site occupancy on the various attributes of Kadcyla® are unknown.

Here, we present results of our extensive characterization of ado-trastuzumab emtansine by a combination of analytical methods. Our aims were to: 1) explore and compare a set of analytical methods that are specific and sensitive to determine the structures of ado-trastuzumab emtansine manufactured by 2 different companies; 2) compare the analytical results and thereby assess the structural similarity of the samples; and 3) evaluate the bioactivity and the cytotoxicity of the ado-trastuzumab emtansine, thus contributing to the analytical strategies for monitoring the development of ADCs and their biosimilars. It is important to note that the conjugation procedure applied for the biosimilar ADC was the same as the documented procedure for the marketed ADC,[23] so we can eliminate any variables that could be caused by different conjugation chemistry. We also report comparisons of LC/MS results for the ADC samples on their primary amino acid sequence, DARs, conjugation sites and site occupancy. Furthermore, thermal stability, free drug content, and impurities were analyzed to further evaluate the 2 ADCs. Lastly, the biological activities of Kadcyla® and the biosimilar ADC were compared using a cytotoxic activity assay and a HER2-binding assay.

Results

Intact MS analysis

ADCs are a complex mixture of conjugated species, which differ in the number of payloads attached as well as the attachment sites of the payload on the mAb. Fig. 1 shows the representative structure of Kadcyla®, in which the modification of lysines on trastuzumab with the succinimidyl 4-(N-maleimidomethyl) cyclohexane-1-carboxylate (SMCC) linker allows the subsequent reaction with the sulfhydryl of the DM1 drug. The distribution of the payload was determined by intact mAb LC/MS analysis. To reduce the complexity of the ADC molecules, ADC samples were treated with PNGase F to remove the N-glycans. After the de-glycosylation step, samples from either Kadcyla® or a candidate biosimilar ADC were analyzed by reversed phase (RP) LC/MS. Fig. 2 shows the raw mass spectra with a m/z range between 2200 and 3600 and the MaxEnt 1 deconvoluted mass spectra for Kadcyla® and the candidate biosimilar ADC. The deconvoluted mass spectrum of Kadcyla® displayed 9 major peaks with a mass difference of 957 Da observed between adjacent peaks. This mass difference matches the combined mass of a covalently linked DM1 drug with one MCC linker (DM1+ MCC, Monoisotopic Mass 956.213 2a). Each mass of the 9 major peaks in both deconvoluted spectra (Kadcyla® and candidate biosimilar ADCs) corresponds to the mass of trastuzumab with 0 to 8 DM1 payloads and linkers, respectively (labeled as +0, +1, etc). For each major peak in the deconvoluted spectra, a lower intensity peak with 220 Da shift was also observed. These smaller peaks were attributed to the linkers that are conjugated to the mAb molecules, but had not reacted with DM1 payloads.[7] The ion intensity between the corresponding MS peaks (by mass) in the spectra differs slightly between the 2 samples, which could be caused by the slight mass load differences in the RP column. Average DARs were determined by the weighted peak areas of all the peaks in the MS profiles. The MS-derived DAR value from ado-trastuzumab emtansine (Kadcyla®) is 3.53 ± 0.05, which agrees very well with reported values.[7] The candidate biosimilar ADC showed a slightly lower DAR value of 3.39 ± 0.01.

Identification of conjugation sites by peptide mapping approach

Lysine-conjugated ADC and unconjugated mAb were treated separately by either trypsin or Asp-N. The digests were separated by RP chromatography and followed by UV and MS analysis in tandem for peptide identification. For each digest, fragmentation data were collected both in data-independent acquisition (MS^E) mode and in data-dependent acquisition (DDA) modes to acquire sequence information about the observed peptides. For low abundant conjugated peptides, MS^E and DDA spectra can jointly identify the conjugate peptides and locate the conjugation sites. Fig. 3 shows the comparative (mirror) plots of LC-MS^E tryptic peptide maps from the Kadcyla® and biosimilar ADC digests in either MS base peak

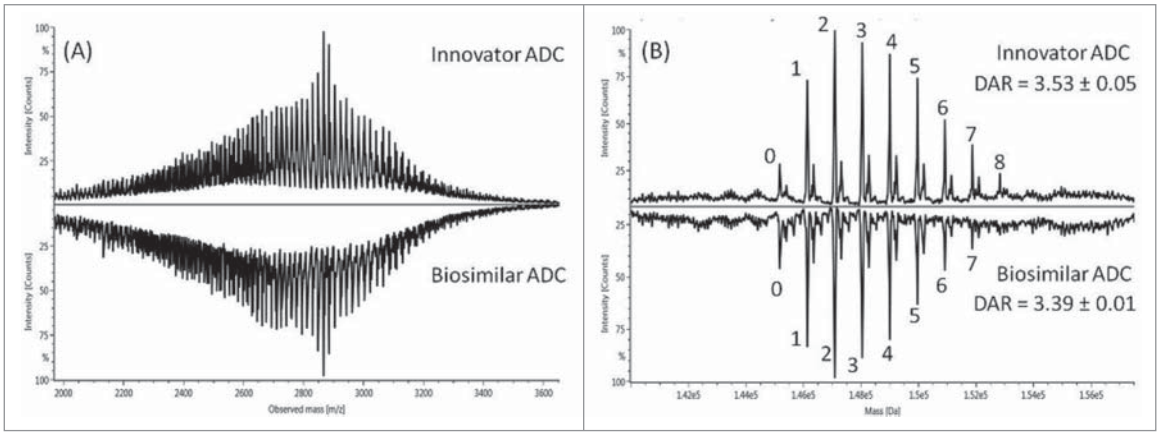

Figure 2. Intact mass spectra comparison between the deglycosylated Kadcyla® and the deglycosylated biosimilar candidate ADC: (A) the combined raw mass spectra with m/z range of 2200-3600 (B) deconvoluted mass spectra (processed by UNIFI 1.8 using MaxEnt1). Both ADC samples were treated with PNGase F. The labeled number 0, 1, …, *n* corresponds to the number of DM1 molecules that are connected to trastuzumab through the linker. The average DAR values are calculated and shown on the plot.

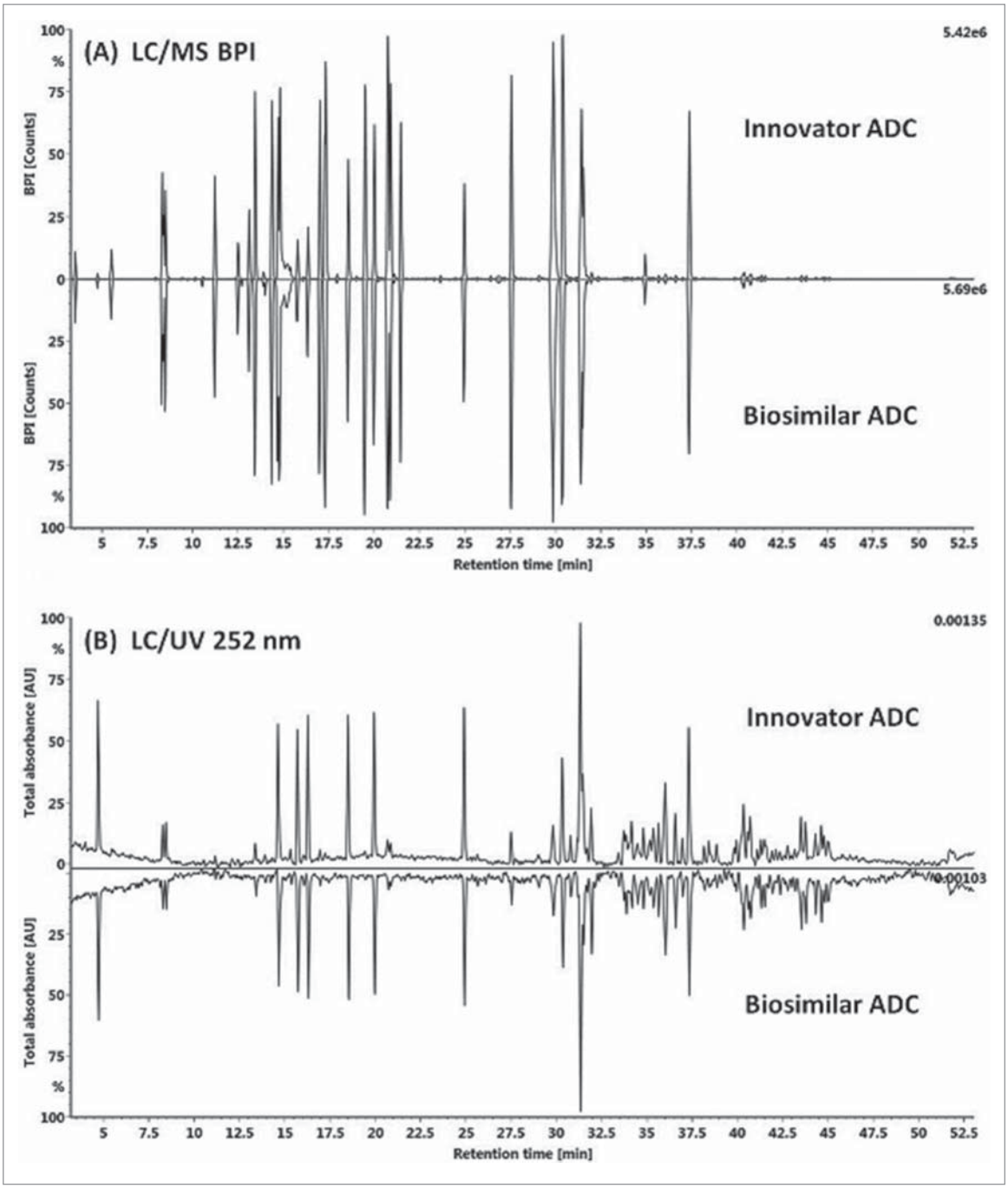

Figure 3. Comparison mirror plots of tryptic peptide maps of Kadcyla® and candidate biosimilar ADC samples. (A) LC/MS^E base peak intensity chromatogram (BPI) (B) LC/UV chromatogram (@ 252 nm).

chromatogram (Fig. 3A) or UV absorbance chromatogram at 252 nm (Fig. 3B). All the conjugated peptides elute later in the gradient and appear from 30 min to 52 min in the chromatogram, due to their increased hydrophobicity caused by the payload moiety.

Upon conjugation, modified lysine residues are no longer trypsin cleavable. As a result, the majority of the tryptic peptides with conjugated payloads are peptides containing one missed trypsin cleavage site, with the exception of lysine followed by a proline; however, the peptides from Asp-N digestion typically do not contain missed cleavages. Therefore, a majority of the conjugated peptides from trypsin digestion encompass a single conjugated lysine (unless it was next to a C-terminal proline), whereas Asp-N digestion can generate peptides with multiple lysine residues (up to 9), creating a mixture of Asp-N peptides with the identical sequence but different conjugation sites (positional isomers). These positional isomers can complicate the determination of the specific conjugated Lys residues, and require more complete sequence coverage in the high energy fragmentation spectrum. For all identified conjugation sites, only partial modification with drug payloads were observed, i.e., both modified and unmodified peptides were discovered in the experiment. Overall, lysine conjugation

Table 1. Summary table of lysine conjugation sites identified in ado-trastuzumab emtansine. Two retention times in the table correspond to 2 diastereomer peaks for each conjugated peptide. Kadcyla® and the candidate biosimilar exhibit the same conjugation sites. * conjugation of DM1 is located on the N-terminal amine group..

	Conjugated Lys Position	Tryptic Peptide	Sequence	RT (min)		Therotical M+H+(Da)	Mass error (ppm)
Light Chain	N-term NH2	1:T1	*DIQMTQSPSSLSASVGDR	41.98	42.38	2835.2506	0.9
	42	1:T3-4	ASQDVNTAVAWYQQKPGKAPK	33.77	34.21	3243.5474	2.7
	45	1:T4-5	APKLLIYSASFLYSGVPSR	47.18	47.42	3025.5074	0.1
	103	1:T7-8	SGTDFTLTISSLQPEDFATYYCQQ HYTTPPTFGQGTKVEIK	41.49	41.77	5613.5723	0.4
	107	1:T8-9	VEIKR	36.09	36.62	1600.7734	−1.1
	126	1:T10-11	TVAAPSVFIFPPSDEQLKSGTASVVCLLNNFYPR	51.80	52.00	4681.2688	1.4
	145	1:T12-13	EAKVQWK	37.02	37.49	1844.8582	−0.9
	149	1:T13-14	VQWKVDNALQSGNSQESVTEQDSK	37.93	38.26	3633.6344	−0.9
	169	1:T14-15	VDNALQSGNSQESVTEQDSKDSTYSLSSTLTLSK	38.49	38.93	4576.0738	0.1
	183	1:T15-16	DSTYSLSSTLTLSKADYEK	41.14	41.49	3065.3878	1.8
	188	1:T16-17	ADYEKHK	31.38	31.99	1846.8011	−3.0
	190	1:T17-18	HKVYACEVTHQGLSSPVTK	30.84	31.23	3097.4452	−3.9
	207	1:T18-19	VYACEVTHQGLSSPVTKSFNR	35.70	36.02	3336.5358	−2.3
Heavy Chain	N-term NH2	2:T1	*EVQLVESGGGLVQPGGSLR	44.67	45.03	2838.3673	−0.1
	30	2:T2-3	LSCAASGFNIKDTYIHWVR	41.35	41.55	3194.4769	2.7
	43	2:T4-5	QAPGKGLEWVAR	39.99	40.38	2268.0812	−2.0
	65	2:T7-8	YADSVKGR	35.40	35.96	1851.8277	−1.1
	76	2:T9-10	FTISADTSKNTAYLQMNSLR	39.88	40.28	3217.4875	1.2
	124	2:T12-13	WGGDGFYAMDYWGQGTLVTVSSASTKGPSVFPLAPSSK	46.32	46.65	4908.2543	−0.4
	136	2:T13-14	GPSVFPLAPSSKSTSGGTAALGCLVK	42.82	43.23	3445.6713	−2.2
	208	2:T15	DYFPEPVTVSWNSGALTSGVHTFPAVLQ SSGLYSLSSVVTVPSSSLGTQTYICNVNHKPSNTK	43.58	43.82	7669.6789	−3.1
	213	2:T15-16	DYFPEPVTVSWNSGALTSGVHTFPAVLQSSGLYSLSS VVTVPSSSLGTQTYICNVNHKPSNTKVDK	41.96	42.20	8011.8692	−3.1
	216	2:T16-17	VDKK	34.43	35.09	1445.6676	−0.6
	217	2:T17-18	KVEPK	34.23	34.86	1556.7360	−1.0
	225	2:T19-20	SCDKTHTCPPCPAPELLGGPSVFLFPPKPK	40.40	40.78	4291.0066	−1.3
	249	2:T20	THTCPPCPAPELLGGPSVFLFPPKPK	44.86	45.11	3800.8220	2.2
	251	2:T20-21	THTCPPCPAPELLGGPSVFLFPPKPKDTLMISR	43.45	43.69	4617.2384	−1.6
	277	2:T22-23	TPEVTCVVVDVSHEDPEVKFNWYVDGVEVHNAK	40.62	40.76	4754.1760	−2.5
	291	2:T23-24	FNWYVDGVEVHNAKTKPR	34.86	35.23	3116.4629	−2.6
	293	2:T24	TKPR	34.04	34.67	1457.6788	−1.4
	320	2:T26-27	VVSVLTVLHQDWLNGKEYK	43.49	43.77	3184.5718	0.5
	323	2:T27-28	EYKCK	33.91	34.55	1683.7088	−0.9
	325	2:T28-29	CKVSNK	33.50	34.12	1691.7462	−1.1
	329	2:T29-30	VSNKALPAPIEK	38.21	38.62	2223.1061	−1.6
	337	2:T30-31	ALPAPIEKTISK	40.26	40.64	2224.1265	−1.6
	341	2:T31-32	TISKAK	34.94	35.35	1603.7731	−0.3
	343	2:T32-33	AKGQPR	33.84	34.49	1612.7483	−0.1
	363	2:T35-36	EEMTKNQVSLTCLVK	40.20	40.62	2736.2624	4.0
	395	2:T37-38	GFYPSDIAVEWESNGQPENNYKTTPPVLDSDGSFFLYSK	44.37	44.71	5355.3998	−1.1
	417	2:T39-40	LTVDKSR	36.07	36.63	1774.8375	−0.9
	442	2:T41-42	WQQGNVFSCSVMHEALHNHYTQKSLSLSPG	36.81	37.06	4398.9700	−2.2

sites identified by the 2 enzymatic digestions were consistent (Table 1).

It is interesting to note that the conjugation sites found in the biosimilar ADC are consistent with sites in Kadcyla®. Table 1 summarizes the conjugation sites identified in Kadcyla® and the biosimilar ADC. For ado-trastuzumab emtansine, there are 92 possible conjugation sites available (88 lysine residues and 4 N-terminal amine groups), of which 82 sites were confirmed to be partially conjugated. Furthermore, 3 sites containing just conjugated linkers were identified (Table 2). They are located at heavy chain K136, K213, and K225, where peptides modified by MCC linker, but not with DM1, were discovered.

The complementarity-determining region (CDR) region of trastuzumab contains one lysine residue, which is located at the heavy chain K^{65}. Both trypsin and Asp-N peptide mapping analysis confirm that the heavy chain K^{65} site is partially occupied by the DM1 payload. MS/MS spectra from tryptic peptide and Asp-N peptide containing the conjugated K65 site are shown in Fig. 4. The collision-induced dissociation fragmentation spectra of the conjugated peptides show a series of signature fragments at m/z of 547.221, 485.224, and 453.199. These signature fragment peaks all show typical isotope patterns produced by compounds containing halogen elements, suggesting these peaks are derived from the chlorine-containing DM1 drug. Conjugated peptides from ado-trastuzumab emtansine also show another characteristic chromatographic behavior that is important to consider for identifying conjugated peptides. Peptides with the conjugated DM1 drug are eluting in pairs, which attributes to the different stereochemical configurations caused by the antibody-drug linkage through a maleimide.[7] Fig. 5 shows the extracted ion chromatogram comparison of the CDR region peptide (^{62}DSVKGRFTISA^{72}) from Asp-N digestion between Kadcyla® and the biosimilar ADC in its conjugated or native form. The diastereomers of the conjugated peptide showed 2 peaks at 40.13 and 40.55 min, respectively, as shown in Fig. 5 (B). The percentages of the conjugated peptides were calculated to be 24 ± 0.04% and 19 ± 0.01% for Kadcyla® and the biosimilar ADC, respectively.

Table 2. Summary table of MCC linker-only sites identified in ado-trastuzumab emtansine. Kadcyla® and the candidate biosimilar show both samples have exactly same linker-only sites.

	Trypsin Digest					Asp-N Digest				
Unreacted linker conjugated Lys Site	Peptide	mass (Da)	RT (min)		Mass error (ppm)	Peptide	mass (Da)	RT (min)		Mass error (ppm)
HC136	2:T13-14	2708.3964	29.40	29.52	−1.8	Not observed				
HC213	2:T15-16	7274.5943	37.55	37.68	2.0	2:D8	7031.4724	38.76	38.95	2.3
HC225	2:T19-20	3553.7317	30.87	31.43	0.3	2:D10	3306.6690	31.65	32.23	1.0

Quantification of the conjugated peptides

To access the conjugation level of Kadcyla® and the biosimilar ADC at the individual site, the intensity of each conjugated tryptic peptide was used for comparison. A known amount of peptide (leucine enkephalin, sequence YGGFL) was spiked into each sample as the internal standard to normalize the MS signal intensity of conjugated peptides between runs. Relative intensities of the identified tryptic conjugated peptide are shown in Fig. 6. The quantification results were grouped and presented according to different domains of antibodies. Fig. 6(A),(B) and (C) present variable domains (V_H, V_L), constant regions (C_H1, C_L) and Fc (C_H2 and C_H3) regions, respectively. Since the majority of the tryptic conjugated peptides only contain one payload, we can use the tryptic conjugated peptides to assess the conjugation level at each individual site. The sites with less conjugation for the biosimilar ADC than Kadcyla® are H30 (residue 30 on the heavy chain) in the V_H, L188 (C_L), H216 (C_H1), H323, H363, and H417 (C_H2+C_H3). In contrast, L145 (C_L) and L169 (C_L) and H337 (C_H2) show slightly higher percentages of conjugation in biosimilar ADC samples.

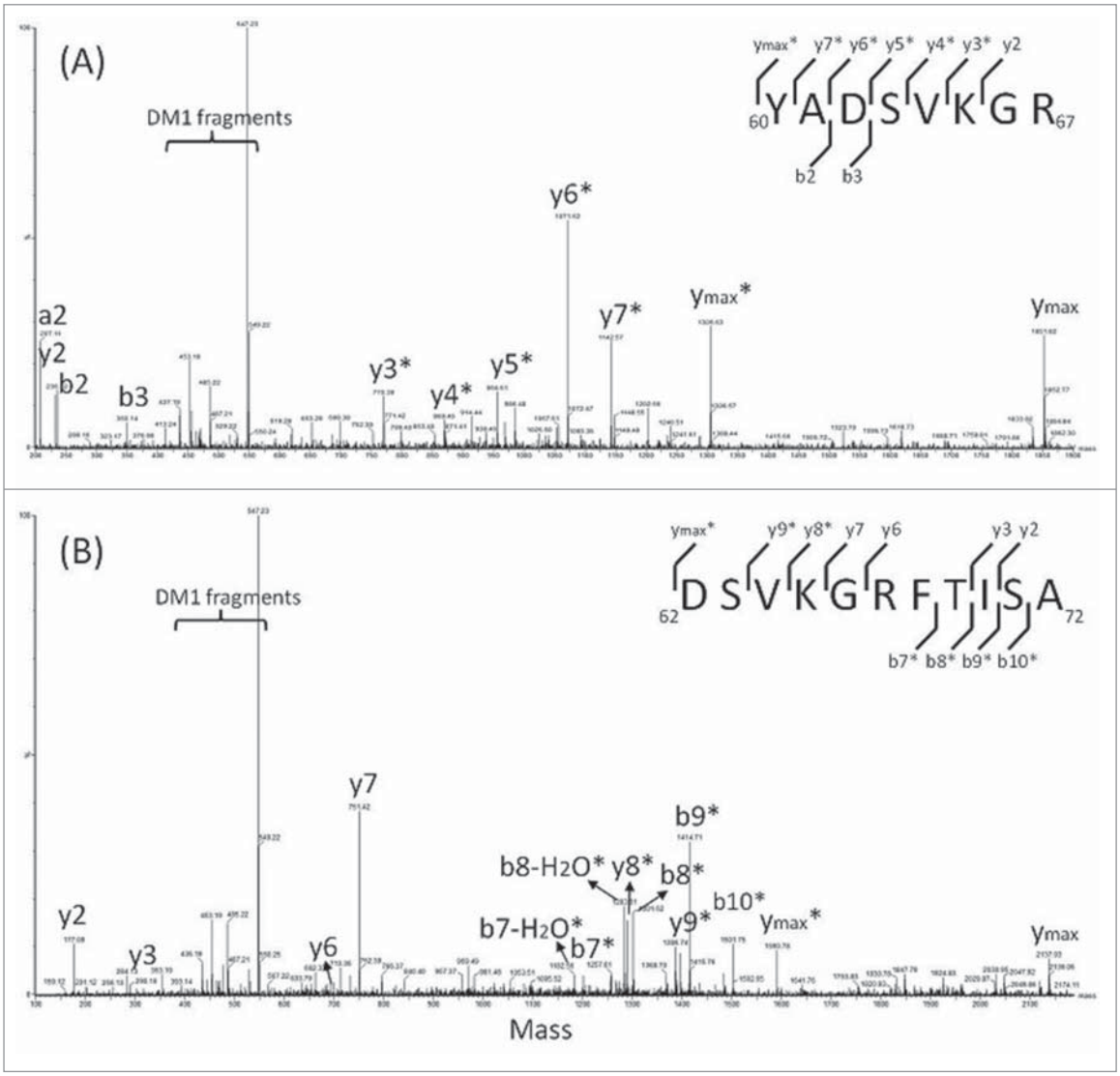

Figure 4. Deconvoluted fragmentation spectra of peptides containing lysine site K65. (A) tryptic peptide HC60-67 (B) Asp-N peptide HC62-72.

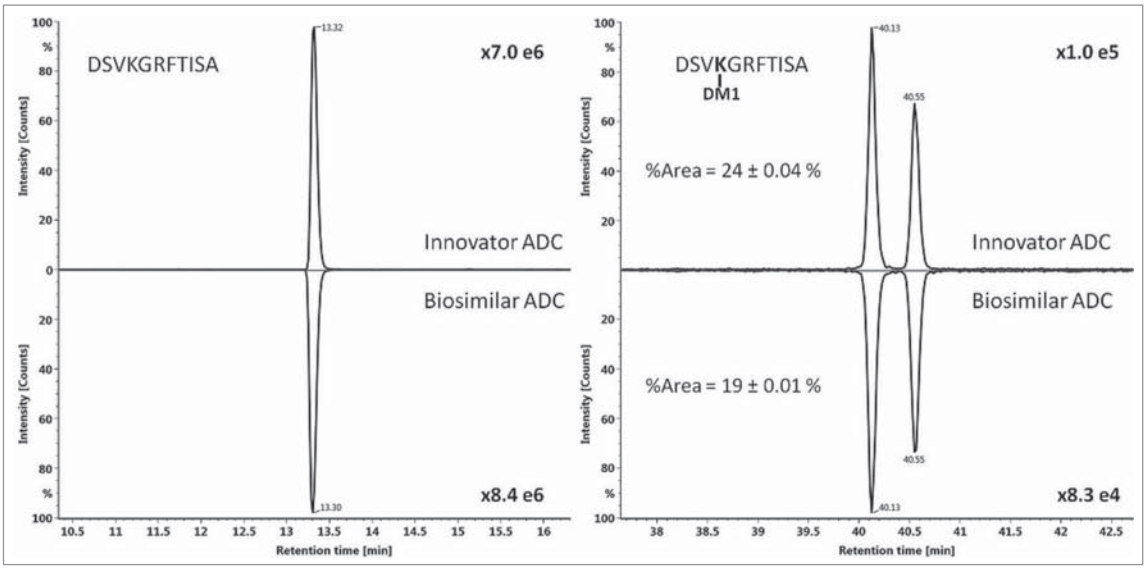

Figure 5. Mirror plots of extracted ion chromatograms (XIC) of the unconjugated and conjugated peptides from the CDR region of trastuzumab covering residue lysine K^{65}. The peptides were from Asp-N digestion of Kadcyla® and the biosimilar ADC samples. The relative peak areas of the conjugated peptides are calculated and labeled on the plot.

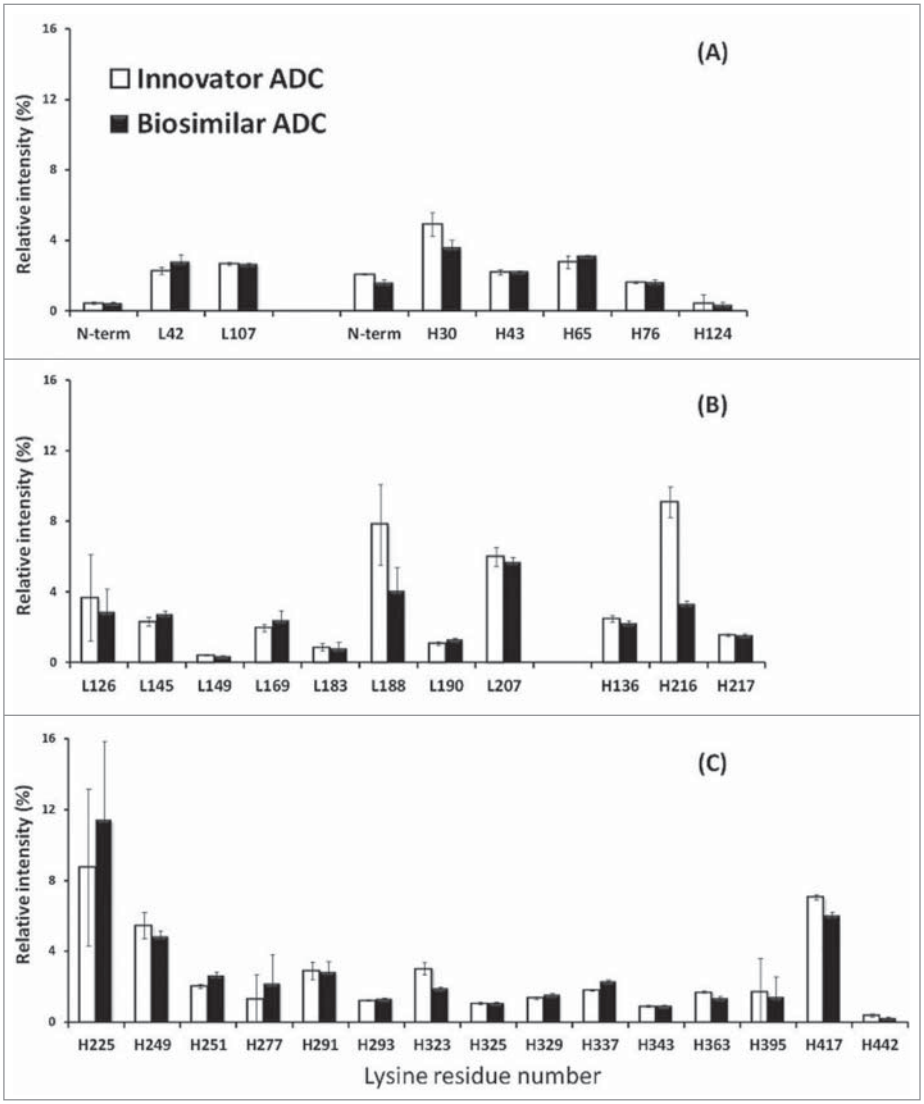

Figure 6. Relative peak areas of the conjugated peptides from tryptic digestion comparing Kadcyla® and the biosimilar candidate ADC. The site of lysine conjugation is labeled on the X axis. The intensity of the conjugated peptides is plotted according to their distribution on trastuzumab: the conjugated peptides from variable domains (V_H, V_L) (A); the conjugated peptides from constant regions (C_H1, C_L) region (B); and the conjugated peptides from Fc (C_H2 and C_H3) regions (C). The reported errors in the figure are due to run-to-run variability.

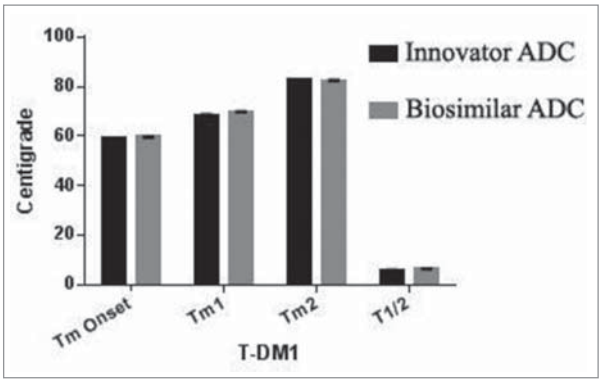

Figure 7. The thermal stabilities of Kadcyla® and the biosimilar candidate ADC were evaluated and compared based on the transition temperature measurement from DSC analysis.

Higher order structures

The thermal stability of Kadcyla® and biosimilar ADCs were evaluated by differential scanning calorimetry (DSC). All the ADC samples were analyzed in the same buffer solution with a concentration of 1 mg/ml. The DSC thermograms for all the ADC samples are displayed in Fig. 7. There were 2 major transitions observed for all the samples. Both transition temperature 1 (Tm1) and transition temperature 2 (Tm2) are similar between Kadcyla® and the biosimilar ADC, which suggests the existence of a similar stability between the 2 samples.[24,23]

Size variants

The size heterogeneity of the ADC samples was determined by 2 orthogonal methods, size-exclusion chromatography (SEC) and capillary electrophoresis-sodium dodecyl sulfate (CE-SDS). SEC analysis results (Fig. 8A) showed that the Kadcyla® sample contains 98.34% (with standard deviation (SD) of 0.04%) of monomer, 1.64% of aggregates (with SD of 0.04%) and 0.02% (with SD of 0.00%) of fragments. In comparison, the biosimilar ADC sample has 97.96% (with SD of 0.03%) of monomer, 2.00% (with SD of 0.03%) of aggregate and 0.04% (with SD of 0.00%) of fragment. Results from non-reduced CE-SDS (Fig. 8B) analysis showed the percentage of monomer is 96.63% (with SD of 0.07%), fragments 2.74% (with SD of 0.02%) and aggregate 0.63% (with SD of 0.06%) in the Kadcyla® sample. For the biosimilar ADC sample, the percentage of monomer is 95.43% (with SD of 0.08%), fragments 3.43% (with SD of 0.07%) and aggregates 1.14% (with SD of 0.13%). Results from both SEC and non-reduced CE-SDS analyses exhibit predominant monomer contents (>95 %) in Kadcyla® and the biosimilar ADC sample. The similar relatively low content of aggregates of Kadcyla® and the biosimilar ADC indicates their similarity in the aspect of size heterogeneity.[25]

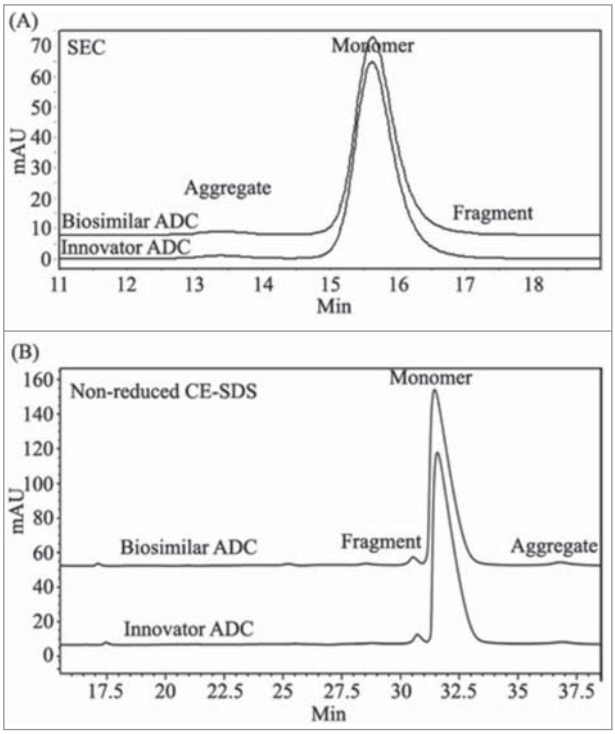

Figure 8. Size variants were accessed with SEC (A) and non-reduced CE-SDS (B); the percentage of monomers between Kadcyla® and the biosimilar ADC are compared.

Unconjugated (Free) drug analysis

Because the small molecule drug payload in an ADC sample is generally highly potent and very toxic, the quantity of unconjugated (free) drug is an important product quality attribute that is directly related to product toxicity and patient safety. The final product may contain residual free drug or drug-related impurities as the result of incomplete removal or shedding. It is therefore essential to characterize and quantify free drug content. Quantitative analysis of DM1 in human serum was previously demonstrated by on-line solid phase extraction with liquid chromatography tandem mass spectrometry.[26] In this study, quantification of free drug content in ADC samples was performed by RP chromatography after protein precipitation. The free drug contents of the ADC samples are shown in Table 3. The abundance of free drug content accounts for 1.15 ± 0.05% and 1.33 ± 0.06% in molar ratio for Kadcyla® and the biosimilar ADC, respectively, which indicates a similar level of unconjugated (free) drug content.

Biological activities

In addition to the structural comparison of Kadcyla® and the biosimilar ADC candidate, the biological activities of the ADCs were evaluated and compared using an in vitro cytotoxic activity assay and a HER2 binding affinity assay (surface plasmon

Table 3. Free drug analysis for Kadcyla® and the biosimilar candidate ADC samples using RP-HPLC.

		ADC		
Name	Run	Purity (%)	X ± S	CV(%)
Innovator ADC	1	1.19	1.15 ± 0.05	4.49
	2	1.18		
	3	1.09		
Biosimilar ADC	1	1.36	1.33 ± 0.06	4.46
	2	1.36		
	3	1.26		

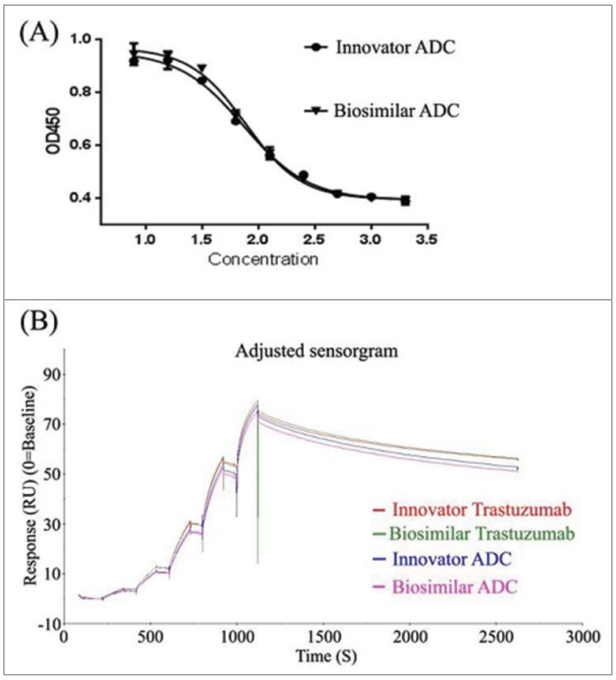

Figure 9. Biological activity analysis of Kadcyla® and the biosimilar candidate ADC. (A) Cell proliferation inhibition assay; (B) HER2-binding assay (BIACORE).

resonance (SPR)). The cell proliferation inhibition assay was performed using human breast cancel BT-474 cells. The results showed that Kadcyla® and the candidate biosimilar ADC exhibited a similar dose-effect relationship. With Kadcyla® as the reference, the cytotoxic activity of candidate biosimilar ADC was measured at 100.54% (Fig. 9A).

To evaluate the effect of linker-DM1 conjugation at the CDR region of trastuzumab on the binding activity to HER2 antigen, the binding of Herceptin®, Kadcyla®, biosimilar trastuzumab and biosimilar ADC to HER2 protein was evaluated by SPR using Biacore T200 (Fig. 9B). The SPR analysis (3 replicates for each sample) showed that a K_d value of 0.8123 nM (with SD of 0.0482) was acquired for Kadcyla® and 0.6858 nM (with SD of 0.0762) for its corresponding unconjugated trastuzumab, while a K_d value of 0.7684 nM (with SD of 0.0234) was obtained for the biosimilar ADC and 0.7371 nM (with SD of 0.0494) for its corresponding unconjugated trastuzumab. The K_D values among the 4 samples are quite similar, which indicates a minimal influence of CDR conjugation on antibody-antigen interaction, and similarity between Kadcyla® and the biosimilar ADC.

Discussion

To define the molecular similarity between a reference mAb and its biosimilar candidate, different LC-MS based approaches have been successfully applied.[21,27] Due to the additional heterogeneity caused by the conjugation, ADCs exhibit an increased level of complexity compared with conventional antibodies. To demonstrate molecular and product equivalency of an ADC biosimilar with a reference ADC product such as Kadcyla®, advanced and more sensitive analytical technologies are needed. In this study, a detailed structural characterization, including intact mass analysis, DAR measurement, conjugation site identification, and site occupancy, was performed to determine the molecular similarity between Kadcyla® and a biosimilar ADC candidate. To examine other product attributes between the candidate biosimilar ADC and Kadcyla®, we applied a series of physicochemical and biological methods to compare high order structure, product impurity, free drug content, and biological activity. The quality attributes considered and analytical techniques we applied are summarized in Table 4.

First, intact mass analysis enabled rapid examination and comparison of the mass, general drug load/distribution pattern and average DAR values between Kadcyla® and the biosimilar ADC. DAR is one of the most important product quality attributes of an ADC. It determines the amount of drug that can be delivered to the target cell, which directly affects safety and efficacy. Depending on the conjugation chemistry and the types of ADCs, different strategies have been implemented for DAR measurement, including UV/Vis,[9] MALDI-TOF-MS,[28] capillary iso-electric focusing (cIEF),[29] CE-MS,[30] HIC,[31] SEC/ESI-MS,[25] and IMMS.[17,18] One advantage of MS-based analysis of ADCs is its independence of the spectroscopic nature of the linker and payload. Lysine-conjugated ADCs represent a substantial challenge for DAR determination due to their high level of heterogeneity. To date, a limited number of studies have reported DAR characterization of lysine-conjugated ADCs. Intact mass spectra clearly demonstrated that Kadcyla® is a mixture of species with a different number of payloads ranging from 0 to 8. The slight difference in DAR observed in the intact mass analysis suggests that the average number of payloads per antibody is slightly different between the biosimilar ADC (3.39 ± 0.01) and Kadcyla® (3.53 ± 0.01). This variation could be caused by the difference in conjugation sites or site occupancy between the samples. DAR values are calculated from the relative MS intensity of the conjugated antibodies and unconjugated antibodies. The difference in ionization efficiency between the naked antibody and the conjugated antibody may cause the MS-derived DAR to be different from the true DAR in some cases. However, the MS-derived average DAR for lysine conjugates correlates well to the UV-derived conjugates as shown in the literature.[7,32] Hence, DAR determined by RP-LC/MS can be used for lot-to-lot comparisons of lysine conjugates.

Table 4. Quality attributes examined and analytical methods applied in this paper.

Attribute	Target	Method applied
Drug distribution	Conjugates	UPLC-MS intact analysis
Drug-to-antibody ratio (DAR)	Conjugates	UPLC-MS intact analysis
Primary sequence	mAbs	UPLC-MS peptide mapping analysis
Site of conjugation/ occupancy	Conjugates	UPLC-MS peptide mapping analysis
Free (unconjugated) drug	Drug	UPLC
Size variants (Aggregates, fragments)	mAbs, conjugates	Size exclusion chromatography, capillary electrophoresis-SDS
High order structure	Conjugates	Differential scanning calorimetry
Bioactivity	Conjugates	Cell proliferation inhibition assay, surface plasmon resonance

Peptide mapping is routinely used to confirm the amino acid sequence and characterize post-translational modifications for antibodies and other recombinant proteins.[33] There are very few studies in the literature that report details about the conjugation sites of ADCs and the site occupancy, especially lysine-conjugated ADCs.[8,29] Conjugation sites of huN901-DM1, another humanized IgG1 antibody with DM1 conjugated to lysine residues by the similar linker chemistry, were reported by Wang et al.[8] Of 86 lysine residues, 40 different sites on the IgG1 antibody were identified with covalently-linked DM1. In a study by Luo et al., 76 lysine sites were identified with the payload for an antibody-DM1 conjugate.[29] As described here, we identified 82 conjugated lysine sites on Kadcyla®, including the 4 N-terminal amine groups from the 2 light chains and the 2 heavy chains of trastuzumab. This data indicates that nearly 90% of lysine residues (a total of 92 primary amine sites) that could possibly be modified by the DM1 drug were conjugated to a certain degree. In addition, among the 82 conjugated sites identified, 3 sites were found partially conjugated with both the DM1-MCC and the MCC linker-only, and all the 3 sites are located on the heavy chain. The existence of ADC species that contain some MCC linker-only sites was also supported by intact mass analysis (Fig. 2), in which peaks with additional 220 Da were observed next to each of the primary peaks. The incomplete conjugation in the second conjugation step of a 2-step conjugation process, where linker-modified intermediates reacted with DM1, may contribute to the linker-only sites present on the antibody.[7] In addition, early studies suggested that tyrosine and histidine residues can also be modified by succinimide ester.[34] However, we did not observe any evidence of tyrosine or histidine residues modified by linker or DM1 drugs in this study.

All the lysine residues in C_H2 domain were modified with the drug at various levels. This observation is consistent with a previous report showing that the lysine residues in the C_H2 domain for IgG1 exhibit a high degree of solvent accessibility and flexibility.[8] Two lysine residues, K^{221} and K^{225}, are located in the hinge region of trastuzumab. However, lysine 221 residue was not found to be modified by the linker or the linked-payload in the study. Overall, 4 other lysine residues on the trastuzumab half body (one light chain and one heavy chain) did not show any signs of conjugation. Of those 5 sites, one lysine was located in the V_L (Light chain K^{39}) region, 2 residues in the C_H3 region (Heavy chain K^{373} and K^{412}), one in the C_H1 (Heavy chain K^{150}) and one in the hinge region (Heavy chain K^{221}). The absence of the conjugated peptides from the 5 sites may be attributed to the low signal intensities of those peptides that are beyond the detection limit of current LC/MS methods. The observation suggests the conjugation level at these sites is likely significantly lower than that at the other identified sites, although we cannot exclude that MS responses from the conjugated peptides may also play a role in the detection.

The CDR of trastuzumab contains one lysine residue (Heavy chain K^{65}), which was also found to be partially modified (Table 1). Without accounting for the ionization efficiency difference between the conjugated peptides and the unconjugated peptides, it is difficult to obtain an accurate picture of the site occupancy (the molar ratio) of the CDR lysine site. Modifications in the CDR region can potentially have an effect on the binding properties of the antibody.[35] It is not unreasonable to assume the HER2 binding ability might be affected somewhat by the alteration of the CDR region caused by the conjugated payload drug. The SPR analysis showed that the binding affinity to the HER2 antigens is to be similar between the naked trastuzumab and DM1-conjugated samples, both for Kadcyla® and the biosimilar ADC. This suggests that the steric hindrance applied by the payload moiety or the degree of the modification at the particular lysine site has not altered the interaction with HER2 antigens to such a degree that SPR can detect. The exact effect of conjugated of CDR lysine sites on the binding affinity needs to be studied in a more controllable manner, and is beyond the scope of this study. However if the lysine site(s) in the CDR is prone to be modified during ADC preparation, the abundance of the CDR peptides seems to be an important attribute to consider to ensure product quality and manufacturing consistence.

It is worth noting that the exact same lysine sites that bear both the conjugated MCC linker-only and the conjugated MCC liner-payload moieties were identified for both Kadcyla® and the biosimilar ADC, indicating a certain level of consistency of the controlled conjugation process. However, comparison of the relative abundance of all the conjugated peptides/sites revealed a degree of variation in the levels of conjugation between Kadcyla® and the biosimilar ADC as shown in Fig. 6 (B). More specifically, the C_L and C_H1 region showed the most significant difference (about 25%) between Kadcyla® and the biosimilar candidate, whereas the V_L, V_H, C_H2 and C_H3 regions had no significant differences.

Although there is no feasible way to directly correlate the DAR value with the abundance of conjugated peptides at an individual site, the overall abundance of all the identified conjugated peptide can be used to compare the conjugation levels in 2 ADC samples along with the average DAR comparison. In this study, the DAR for biosimilar candidate ADC ($3.39 \pm 0\ .01$) was slightly less than Kadcyla® ($3.53 \pm 0\ .05$), which is consistent with the results from peptide analysis, where slightly lower abundance of conjugated peptides for the biosimilar candidates was observed than for Kadcyla®. Although the DAR value of Kadcyla® and the biosimilar ADC differs somewhat from each other, this statistically significant difference does not cause biological activity differences in terms of cytotoxic activity and antigen-binding activity. Since the molecular similarity should be carefully assessed and closely monitored during biosimilar ADC development, the acceptance criteria based on physiochemical parameters like the DAR value or conjugation level should be set to correlate with comprehensive biological activity assays for the molecular similarity assessment.

DSC measures thermal stability of proteins or antibodies by quantifying the thermal denaturation process. Thermal stability can be used to determine the melting temperature, stability, and purity of a given sample.[36] DSC is widely used for evaluation of pharmaceutical products.[37] The specific application of DSC to the characterization of mAbs has been discussed previously.[38] Such applications include formulation optimization studies,[39] the comparison of the reference product and biosimilar ADCs,[21] the determination of the stabilizing effect of specific oligosaccharide PTM on mAbs,[40] and pH dependence of conformational change.[38] It was demonstrated in the study by

Ionescu et al. [17] that the first transition (Tm1) in trastuzumab represents the unfolding of the CH2 domain, while the second transition represents melting the C_H3 and the Fab regions.[24] The decrease in Tm1 was observed for trastuzumab and Kadcyla®, which decreased by ~3.2°C, while the decrease in Tm2 was only ~0.1°C (data not shown). The findings were consistent with the previous study, suggesting the conjugation of trastuzumab with DM1 has a greater effect on the thermal stability of the C_H2 domain than that shown by the rest of the antibodies.[23] The 2 similar transition temperatures, Tm1 and Tm2, between Kadcyla® and the biosimilar candidate ADC suggest that the 2 samples have similar thermal stability.

The level of aggregation of Kadcyla® and trastuzumab was dramatically different as demonstrated in a previous study.[23] The modification of the surface lysine residues with a large hydrophobic molecule like DM1 results in neutralization of the positive charge and a significant increase in the hydrophobicity of the molecule. Since ado-trastuzumab emtansine is prone to aggregation, monomer content has to be closely monitored due to process change or during manufacturing. SEC-HPLC and CE-SDS demonstrated the monomer content to be similar or lower in the biosimilar ADC compared with Kadcyla®.

In summary, we presented a detailed structural characterization of ado-trastuzumab emtansine, including establishing the drug load profile. We also succeeded in localizing and profiling the individual drug conjugation site. The structural characteristics between a biosimilar candidate ADC and the brand product Kadcyla® were compared to define molecular similarity. This study demonstrated that the 2 ADCs are structurally quite similar, although a discrepancy was found in DARs and the conjugation ratios in some lysine conjugation sites. Since these structural features or the quality attributes are critical to the clinical efficacy and safety of ADC, they need to be closely assessed and monitored during the development of a biosimilar ADC. Furthermore, other product attributes were also compared in this study, including high order structure, monomer content, free drug content, and biological activities. These characteristics between the biosimilar ADC candidate and Kadcyla® match well despite of the discrepancy found in DARs and the conjugation ratios. However, properties like plasma stability and in vivo pharmacokinetics have not been evaluated in the current study for the ADC samples, which can be different due to the observed difference in DAR values, conjugation ratio or conjugation site distribution.[41] Therefore in the development process of a biosimilar ADC, the structural features should be further studied in relationship to other attributes, especially biological activities, to properly understand the similarity of ADC biosimilar products in the future. In addition, it is also important to choose the appropriate analytical and bioanalytical techniques to assess the similarity of the products and ensure the product quality during manufacturing.

Materials and methods

Sample and materials

Kadcyla® and Herceptin® were from Genentech Roche (Basel, Switzerland), and the candidate trastuzumab and biosimilar ADC were from a Chinese pharmaceutical manufacturer. Iodoacetamide (IAM), dithiothreitol (DTT), urea, tris-hydrochloride (tris-HCl) were purchased from Sigma-Aldrich (St. Louis, MO, USA). Sequencing grade modified trypsin and Asp-N were purchased from Promega Corporation (Madison, WI, USA). Formic acid, acetonitrile (ACN, Optima LC/MS grade) and H_2O (Optima LC/MS grade), and tris hydrochloride solution (1 M, pH 7.5) were obtained from Fisher Scientific (Pittsburg, PA, USA). Illustra NAP-5 columns were purchased from GE Healthcare (Pittsburg, PA, USA).

Intact mass

Herceptin® and Kadcyla® solution were diluted to a concentration of 1 mg/mL in 100 μl 1 M tris-HCl buffer (pH = 7.5). 2 μl of glycerol-free PNGase F (New England BioLabs, Ipswich, MA, USA) solution was added into each sample, and the reaction mixture was incubated for 20 hours at 37°C. The incubated solution was diluted with 3% acetonitrile, 97% H_2O, and 0.1% formic acid to final concentration of 0.5 mg/mL. A total of 0.5 μg of Herceptin® or Kadcyla® was injected for each LC/MS run.

Peptide mapping analysis

Trastuzumab (1 mg/ml) and ado-trastuzumab emtansine (1 mg/ml) were denatured in 6.5 M guanidine chloride, with 0.25 M Tris, and pH of 7.5. The denatured antibody solution was mixed with 500 mM DTT to a final concentration of 3 mM and incubated at room temperature for 45 minutes, then alkylated by adding 500 mM iodoacetamide stock solution to a final concentration of 7 mM incubated at room temperature in the dark for 40 minutes. Buffer exchange (0.1 M Tris, 1 M urea, pH 7.5) was performed using a NAP-5 column (GE Healthcare, Wilmington, MA, USA). Sequencing-grade modified trypsin or Asp-N was added to each sample (enzyme to protein ratio 1:25, w/w) and incubated at 37 °C for 5 hours. The digested peptide mixture was diluted to 0.45 μM. Leucine enkephalin (LeuEnk, sequence YGGFL) was added to the mixture at the final concentration of 0.05 μM. The injection volume for each LC/MS run was 5.0 μl.

LC/MS Instruments and bioinformatics

Intact protein and enzyme digests of trastuzumab and ado-trastuzumab emtansine were analyzed in triplicate using an ACQUITY UPLC H-Class Bio System coupled with a Xevo G2-XS QToF mass spectrometer equipped with a lockspray ion source (Waters Corp., Milford, MA, USA). Intact protein samples were separated with an ACQUITY UPLC protein column (2.1 mm X 50 mm BEH300 C4 1.7 μm, Waters Corp, Milford, MA) using a 10 min linear gradient at a flow rate of 0.200 mL/min. Peptides from protein digests were separated with a ACQUITY UPLC peptide column (2.1 × 100 mm BEH300 C18 1.7 μm, Waters Corp, Milford, MA) using a 60-min linear gradient at a flow rate of 0.200 mL/min. Mobile Phase A was made up of water with 0.1% formic acid, while Mobile Phase B was made up of acetonitrile with 0.1% formic acid. For the data acquisition during the peptide analysis, the Xevo G2 XS QToF mass spectrometer was operated either in the MS^E or FastDDA modes. For the MS^E mode, the instrument alternated between low energy and high energy scans (0.5 sec per scan), which

were used to generate intact peptide ions (from low energy scans) and peptide product ions (from high energy scans). A collision energy ramp between 20 V and 45 V was used for fragmenting peptides in high energy scans. Glu-fibrinopeptide standard (Waters, MA, USA) at a concentration of 100 fmol/ μL (m/z 785.8426) was continuously infused at a flow rate of 10 μL/min through the lockspray channel, and the lockmass signal (for 0.5-sec scan) was acquired at every 30 s to provide the external mass calibration.

The LC/MS raw data for peptide analysis was processed using UNIFI Scientific Informatics System (Version 1.8) to generate precursor masses as well as the associated product ion masses (charge state reduced and de-isotoped) for subsequent protein identification and quantification. The following criteria were used to identify the conjugated peptides during the current analysis: 1) Mass accuracy for the matched precursors must be within 4 ppm of mass error; 2) At least 3 primary fragment ions must be matched for each mass-confirmed peptide; and 3) Signature fragments (m/z, 547.221) must correspond to the drug payload and are observed for identification of conjugated peptides.

For peptide quantification, extracted ion chromatographic (XIC) peak areas that correspond to all the charge states along with all the specified adduct ions of each peptide (e.g., sodiated adducts) were combined as a single measure to quantify the abundance of the peptide and its conjugated isoforms. All the peak areas were normalized against the peak areas of the spiked-in internal standards, and triplet injections were performed for each sample. The relative site occupancy from Asp-N digestion was calculated as the ratio of conjugated peptide peak area and total peptide peak area using Eq. (1):

$$\begin{aligned}\text{Site occupancy} &= \text{Area (conjugated pep. peak)}/ \\ &\quad [\text{Area(conjugated pep. peak)} \\ &\quad + \text{Area (unconjugated pep. peak)}] \end{aligned} \quad (1)$$

Differential scanning calorimetry

Thermal analysis of the ADC samples was performed using MicroCal VP-Capillary DSC. Each ADC sample was diluted to 1.0 mg/ml by addition of phosphate-buffered saline. The instrument scanned each sample over a temperature range of 20 to 110°C at a rate of 1.5°C /min. Data analysis was done using Origin 7.

Free drug analysis

The ADC samples (50 μl each) were treated with 100 μl cold methanol and incubated for 30 min in ice bath. The samples were then centrifuged at 13,000 rpm for 30 min and the supernatant was subject to further analysis using RP liquid chromatography. The standard curve was generated using serial dilution of DM1 standards stock solution. The free DM1 amount was calculated by Eq. (2) as follows:

$$\text{Free DM1 \%} = \text{moles of Free DM1} / (\text{DAR x moles ADCs}) \quad (2)$$

Size-exclusion chromatography

SEC experiments were performed using the Waters Alliance 2690 system using TSKgel G3000SWXL (5μm, 300 × 7.8 mm). The mobile phase was 0.2 M tripotassium phosphate and 15% isopropyl alcohol at a flow rate of 0.5 ml/min. The UV absorbance was measured at a wavelength of 280 nm.

Capillary sodium dodecyl sulfate gel electrophoresis

The Beckman PA800 plus system was used for CE-SDS with Beckman capillary (50 um ID x 65 cm) to analyze the ADCs samples. All samples were diluted to 1.0 mg/ml with water. Fifty μl of each ADC sample was mixed with 100 μl of SDS sample buffer and 5 μl of 500 mM iodoacetamide. The mixture was heated at 70°C for 10 min before injection. The instrument was operated at a voltage of 15 kV for protein separation and the UV detection was recorded at a wavelength of 220 nm.

Cell proliferation inhibition assay

BT-474 cells at the logarithmic growth phase were treated with 0.25% Trypsin-EDTA. Cells were re-suspended in 10% FBS-DMEM / F12 medium with cell density at 1.5×10^5 / ml, and they were seeded in a 96-well cell culture plate (100 μl per well). 1:2 folds of serial dilution of the samples was done using 10% FBS-DMEM/ F12 culture medium to a final concentration of 0.039 μg/ml. The series of diluted samples were transferred into BT-474 cell culture plates that had been inoculated (50 μl per well). The plates were incubated at 37°C in a humidified 5% CO_2 incubator for 5 2. After incubation, each well was treated with 10 μl CCK-8 solution followed by incubation for 4 hours. The absorbance at 450 nm was recorded using a SpectraMax M5 microplate reader.

Surface plasmon resonance

The binding to HER2 protein was evaluated by SPR using Biacore T200. Anti-human IgG-Fc antibodies were immobilized to a CM5 sensor chip surface via the amine coupling method. Each ADC sample was diluted to 5 μg/ml with a 1X HBS-EP buffer with a flow rate of 5 μl/min to flow through Flow Cell 2. The HER2 protein was serially diluted with 1X HBS-EP buffer and injected into the ligand-immobilized CM5 chip with an injection time of 120 seconds and a dissociation time of 1500 2econds. The data was globally fitted using a 1:1 binding model. The K_D value was evaluated using Biacore T200 software (v. 2.0).

Disclosure of potential conflicts of interest

No potential conflicts of interest were disclosed.

Acknowledgment

We wish to thank all participants in the collaborative study for their time and invaluable expert contributions, as this study would not have been possible without their input.

Funding

This work was financially supported by grants from the National Science and Technology Major Project, China (No. 2014ZX09304311-001) and NIFDC Academic Leader Training Fund, China (2013X3).

References

1. Weiner LM. Building better magic bullets — improving unconjugated monoclonal antibody therapy for cancer. Nat Rev Cancer 2007; 7 (9):701–706; PMID:17721434; http://dx.doi.org/10.1038/nrc2209
2. Lambert JM. Drug-conjugated monoclonal antibodies for the treatment of cancer. Curr Opin Pharmacol 2005; 5(5):543–549; PMID:16087399; http://dx.doi.org/10.1016/j.coph.2005.04.017
3. Lewis Phillips GD, Li G, Dugger DL, Crocker LM, Parsons KL, Mai E, Blättler WA, Lambert JM, Chari RV, Lutz RJ, et al. Targeting HER2-positive breast cancer with trastuzumab-DM1, an antibody-cytotoxic drug conjugate. Cancer Research 2008; 68 (22):9280–9290; PMID:19010901; http://dx.doi.org/10.1158/0008-5472.CAN-08-1776
4. Francisco JA, Cerveny CG, Meyer DL, Mixan BJ, Klussman K, Chace DF, Rejniak SX, Gordon KA, DeBlanc R, Toki BE, et al. cAC10-vcMMAE, an anti-CD30-monomethyl auristatin E conjugate with potent and selective antitumor activity. Blood 2003; 102(4):1458–1465; PMID:12714494; http://dx.doi.org/10.1182/blood-2003-01-0039
5. Beck A, Haeuw JF, Wurch T, Goetsch L, Bailly C, Corvaïa N. The next generation of antibody-drug conjugates comes of age. Discov Med 2010; 10(53):329–339; PMID:21034674
6. Beck A, Reichert JM. Antibody-drug conjugates: Present and future. mAbs 2014; 6(1):15–17; PMID:24423577; http://dx.doi.org/10.4161/mabs.27436
7. Kim MT, Chen Y, Marhoul J, Jacobson F. Statistical modeling of the drug load distribution on trastuzumab emtansine (Kadcyla), a lysine-linked antibody drug conjugate. Bioconjugate Chemistry 2014; 25 (7):1223–1232; PMID:24873191; http://dx.doi.org/10.1021/bc5000109
8. Wang L, Amphlett G, Blättler WA, Lambert JM, Zhang W. Structural characterization of the maytansinoid-monoclonal antibody immunoconjugate, huN901-DM1, by mass spectrometry. Protein Sci 2005; 14 (9):2436–2446; PMID:16081651; http://dx.doi.org/10.1110/ps.051478705
9. Wakankar A, Chen Y, Gokarn Y, Jacobson FS. Analytical methods for physicochemical characterization of antibody drug conjugates. mAbs 2011; 3(2):161–172; PMID:21441786; http://dx.doi.org/10.4161/mabs.3.2.14960
10. Beck A, Debaene F, Diemer H, Wagner-Rousset E, Colas O, Van Dorsselaer A, Cianférani S. Cutting-edge mass spectrometry characterization of originator, biosimilar and biobetter antibodies. J Mass Spectrom 2015; 50(2):285–297; PMID:25800010; http://dx.doi.org/10.1002/jms.3554
11. Beck A, Terral G, Debaene F, Wagner-Rousset E, Marcoux J, Janin-Bussat MC, Colas O, Van Dorsselaer A, Cianférani S. Cutting-edge mass spectrometry methods for the multi-level structural characterization of antibody-drug conjugates. Expert Rev Proteomics 2016; 13(2):157–183; PMID:26653789; http://dx.doi.org/10.1586/14789450.2016.1132167
12. Qu M, An B, Shen S, Zhang M, Shen X, Duan X, Balthasar JP, Qu J. Qualitative and quantitative characterization of protein biotherapeutics with liquid chromatography mass spectrometry. Mass Spectrom Rev 2016; PMID:27097288; http://dx.doi.org/10.1002/mas.21500
13. Huang RY, Chen G. Characterization of antibody-drug conjugates by mass spectrometry: advances and future trends. Drug Discov Today 2016; 21(5):850–5; PMID:27080148; http://dx.doi.org/10.1016/j.drudis.2016.04.004
14. Le LN, Moore JMR, Ouyang J, Chen X, Nguyen MDH, Galush WJ. Profiling antibody drug conjugate positional isomers: a system-of-equations approach. Analytical Chem 2012; 84(17):7479–7486; PMID:22913809; http://dx.doi.org/10.1021/ac301568f
15. Birdsall RE, Shion H, Kotch FW, Xu A, Porter TJ, Chen W. A rapid on-line method for mass spectrometric confirmation of a cysteine-conjugated antibody-drug-conjugate structure using multidimensional chromatography. MAbs 2015; 7(6):1036–1044; PMID:26305867; http://dx.doi.org/10.1080/19420862.2015.1083665
16. Goldmacher VS, Amphlett G, Wang L, Lazar AC. Statistics of the distribution of the abundance of molecules with various drug loads in maytansinoid antibody-drug conjugates. Mol Pharm 2015; 12(6):1738–1744; PMID:25635630; http://dx.doi.org/10.1021/mp5007536
17. Marcoux J, Champion T, Colas O, Wagner-Rousset E, Corvaïa N, Van Dorsselaer A, Beck A, Cianférani S. Native mass spectrometry and ion mobility characterization of trastuzumab emtansine, a lysine-linked antibody drug conjugate: Native MS and IM-MS for Trastuzumab Emtansine Analysis. Protein Sci 2015; 24(8):1210–1223; PMID:25694334; http://dx.doi.org/10.1002/pro.2666
18. Huang RYC, Deyanova EG, Passmore D, Rangan V, Deshpande S, Tymiak AA, Chen G. Utility of Ion Mobility Mass Spectrometry for Drug-to-Antibody Ratio Measurements in Antibody-Drug Conjugates. J Am Soc Mass Spectrom 2015; 26(10):1791–4; PMID:26122520; http://dx.doi.org/10.1007/s13361-015-1203-1
19. Luo Q, Chung HH, Borths C, Janson M, Wen J, Joubert MK, Wypych J. Structural Characterization of a Monoclonal Antibody-Maytansinoid Immunoconjugate. Anal Chem 2015; 88(1):695–702; PMID:26629796; http://dx.doi.org/10.1021/acs.analchem.5b03709
20. Birdsall RE, McCarthy SM, Janin-Bussat MC, Perez M, Haeuw JF, Chen W, Beck A. A sensitive multidimensional method for the detection, characterization, and quantification of trace free drug species in antibody-drug conjugate samples using mass spectral detection. MAbs 2015; 8(2):306–17; PMID:26651262; http://dx.doi.org/10.1080/19420862.2015.1116659
21. Jung SK, Lee KH, Jeon JW, Lee JW, Kwon BO, Kim YJ, Bae JS, Kim DI, Lee SY, Chang SJ. Physicochemical characterization of Remsima. mAbs 2014; 6(5):1163–1177; PMID:25517302; http://dx.doi.org/10.4161/mabs.32221
22. Strop P, Liu S-H, Dorywalska M, Delaria K, Dushin RG, Tran TT, Ho WH, Farias S, Casas MG, Abdiche Y, et al. Location Matters: Site of Conjugation Modulates Stability and Pharmacokinetics of Antibody Drug Conjugates. Chem Biol 2013; 20(2):161–167; PMID:23438745; http://dx.doi.org/10.1016/j.chembiol.2013.01.010
23. Wakankar AA, Feeney MB, Rivera J, Chen Y, Kim M, Sharma VK, Wang YJ. Physicochemical Stability of the Antibody—Drug Conjugate Trastuzumab-DM1: Changes due to Modification and Conjugation Processes. Bioconjug Chem 2010; 21(9):1588–1595; PMID:20698491; http://dx.doi.org/10.1021/bc900434c
24. Ionescu RM, Vlasak J, Price C, Kirchmeier M. Contribution of variable domains to the stability of humanized IgG1 monoclonal antibodies. J Pharm Sci 2008; 97(4):1414–1426; PMID:17721938; http://dx.doi.org/10.1002/jps.21104
25. Lazar AC, Wang L, Blättler WA, Amphlett G, Lambert JM, Zhang W. Analysis of the composition of immunoconjugates using size-exclusion chromatography coupled to mass spectrometry. Rapid Communications in Mass Spectrometry 2005; 19(13):1806–1814; PMID:15945030; http://dx.doi.org/10.1002/rcm.1987
26. Heudi O, Barteau S, Picard F, Kretz O. Quantitative analysis of maytansinoid (DM1) in human serum by on-line solid phase extraction coupled with liquid chromatography tandem mass spectrometry - Method validation and its application to clinical samples. J Pharm Biomed Anal 2016; 120:322–332; PMID:26771131; http://dx.doi.org/10.1016/j.jpba.2015.12.026
27. Xie H, Chakraborty A, Ahn J, Yu YQ, Dakshinamoorthy DP, Gilar M, Chen W, Skilton SJ, Mazzeo JR. Rapid comparison of a candidate biosimilar to an innovator monoclonal antibody with advanced liquid chromatography and mass spectrometry technologies. MAbs 2010; 2 (4):379–394; PMID:20458189; http://dx.doi.org/10.4161/mabs.11986
28. Quiles S, Raisch KP, Sanford LL, Bonner JA, Safavy A. Synthesis and preliminary biological evaluation of high-drug-load paclitaxel-antibody conjugates for tumor-targeted chemotherapy. J Med Chem 2010; 53 (2):586–594; PMID:19958000; http://dx.doi.org/10.1021/jm900899g
29. Luo Q, Chung HH, Borths C, Janson M, Wen J, Joubert MK, Wypych J. Structural Characterization of a Monoclonal Antibody-Maytansinoid Immunoconjugate. Anal Chem 2016; 88(1):695–702; PMID:26629796; http://dx.doi.org/10.1021/acs.analchem.5b03709
30. Redman EA, Mellors JS, Starkey JA, Ramsey JM. Characterization of Intact Antibody Drug Conjugate Variants Using Microfluidic Capillary Electrophoresis-Mass Spectrometry. Anal Chem 2016; 88(4):2220–2226; PMID:26765745; http://dx.doi.org/10.1021/acs.analchem.5b03866
31. Hamblett KJ, Senter PD, Chace DF, Sun MM, Lenox J, Cerveny CG, Kissler KM, Bernhardt SX, Kopcha AK, Zabinski RF, et al. Effects of drug loading on the antitumor activity of a monoclonal antibody drug

conjugate. Clin Cancer Res 2004; 10(20):7063–7070; PMID:15501986; http://dx.doi.org/10.1158/1078-0432.CCR-04-0789
32. Boylan NJ, Zhou W, Proos RJ, Tolbert TJ, Wolfe JL, Laurence JS. Conjugation site heterogeneity causes variable electrostatic properties in Fc conjugates. Bioconjug Chem 2013; 24(6):1008–1016; PMID:23777335; http://dx.doi.org/10.1021/bc4000564
33. Zhang Z. Large-scale identification and quantification of covalent modifications in therapeutic proteins. Analytical Chem 2009; 81(20):8354–8364; PMID:19764700; http://dx.doi.org/10.1021/ac901193n
34. Leavell MD, Novak P, Behrens CR, Schoeniger JS, Kruppa GH. Strategy for selective chemical cross-linking of tyrosine and lysine residues. J Am Soc Mass Spectrom 2004; 15(11):1604–1611; PMID:15519227; http://dx.doi.org/10.1016/j.jasms.2004.07.018
35. Haberger M, Bomans K, Diepold K, Hook M, Gassner J, Schlothauer T, Zwick A, Spick C, Kepert JF, Hienz B, et al. Assessment of chemical modifications of sites in the CDRs of recombinant antibodies: Susceptibility vs. functionality of critical quality attributes. MAbs 2014; 6 (2):327–339; PMID:24441081; http://dx.doi.org/10.4161/mabs.27876
36. Chiu MH, Prenner EJ. Differential scanning calorimetry: An invaluable tool for a detailed thermodynamic characterization of macromolecules and their interactions. J Pharm Bioallied Sci 2011; 3(1):39–59; PMID:21430954; http://dx.doi.org/10.4103/0975-7406.76463
37. Clas SD, Dalton CR, Hancock BC. Differential scanning calorimetry: applications in drug development. Pharm Sci Technolo Today 1999; 2 (8):311–320; PMID:10441275; http://dx.doi.org/10.1016/S1461-5347(99)00181-9
38. Ejima D, Tsumoto K, Fukada H, Yumioka R, Nagase K, Arakawa T, Philo JS. Effects of acid exposure on the conformation, stability, and aggregation of monoclonal antibodies. Proteins 2007; 66(4):954–962; PMID:17154421; http://dx.doi.org/10.1002/prot.21243
39. Duddu SP, Dal Monte PR. Effect of glass transition temperature on the stability of lyophilized formulations containing a chimeric therapeutic monoclonal antibody. Pharm Res 1997; 14(5):591–595; PMID:9165528; http://dx.doi.org/10.1023/A:1012144810067
40. Liu H, Bulseco GG, Sun J. Effect of posttranslational modifications on the thermal stability of a recombinant monoclonal antibody. Immunol Lett 2006; 106(2):144–153; PMID:16831470; http://dx.doi.org/10.1016/j.imlet.2006.05.011
41. Bender B, Leipold DD, Xu K, Shen BQ, Tibbitts J, Friberg LE. A mechanistic pharmacokinetic model elucidating the disposition of trastuzumab emtansine (T-DM1), an antibody-drug conjugate (ADC) for treatment of metastatic breast cancer. AAPS J 2014; 16 (5):994–1008; PMID:24917179; http://dx.doi.org/10.1208/s12248-014-9618-3